Journal of Photopolymer Science and Technology
Volume 27, Number 1 (2014) 53 –59 © 2014SPST

A Physics-based Model for Negative Tone Development Materials

Chao Fang[a], Mark D. Smith[a], Stewart A. Robertson[a], John J. Biafore[a], and Alessandro Vaglio Pret[b]

[a]*KLA-Tencor Corp. PSG Division, Austin, TX 78759, USA*
[b]*KLA-Tencor Corp. PSG/ICOS, 3001 Leuven, Belgium*

A simple analysis of aerial image quality reveals that negative tone imaging is superior to positive tone for small dimension contacts and trenches. Negative Tone Development (NTD) of positive chemically amplified (de-protecting) photoresist is currently the favored method for realizing such images on the wafer. One of the challenges for these materials is prediction of cross-section shape. Cross-section shape is often critical in leading-edge lithography processes where resist thinning or top loss can lead to pattern failure during the etch process.

There are two important effects that make prediction of cross-section shape more difficult for NTD materials. First, NTD materials typically do not have the develop contrast of positive tone develop (PTD) systems. NTD often has a larger minimum (unexposed) develop rate, and a smaller maximum (fully exposed) develop rate. Second, photoresist typically shrinks after post-exposure bake in regions where de-protection is high. For PTD, these regions dissolve, and the features are formed by the protected areas which do not show shrinkage. The opposite is true for NTD, where the regions with the largest amount of shrinkage form the features on the wafer.

We demonstrate a photoresist model that incorporates resist shrinkage following the elasticity theory described by Flory – volume loss due to de-protection leads to a stress in the photoresist, and the material deforms in a way that minimizes the free energy of the system. We show that this model, combined with accurate dissolution rate measurements, can accurately predict cross-section shape for isolated and dense trenches formed with an example NTD material.

Keyword: negative tone development, lithography simulation, finite element method, shrinkage

1. Introduction

It has long been known that certain features will print with superior image quality with a negative tone resist process. Mack [1] published on this as early as 1991. Despite this, mass volume manufacturing processes at the 248nm and 193nm wavelengths have almost exclusively utilized positive tone chemically amplified photoresists developed in aqueous base solution. These resists operate on the principal of acid catalyzed de-protection to modulate the polymer solubility in the developer. Although negative tone chemically amplified resists have been developed, for one reason or another, they have never been widely adopted in mainstream IC processing.

In recent years, with the introduction of ArF immersion systems and multiple patterning techniques, the ever-diminishing process windows for back-end features such as contacts and semi-dense trenches have prompted renewed interest in negative tone imaging, because simple aerial image analysis shows substantial benefits from changing from the conventional positive tone imaging.

Received April 2, 2014
Accepted May 15, 2014

Promising results have been shown for these layers utilizing a novel process for producing a negative tone resist image: rather than using the standard cross-linking resist system [2,3] developed in an aqueous base, a standard de-protecting (positive type) resist [4,5] is used with a solvent-based development solution. It has been reported that such negative tone development processes do indeed image with superior quality to the standard positive tone approach [6,7].

Physical simulation of lithography has a long history [8] of aiding researchers and engineers in understanding and optimizing real world processes. Ideally, this would also be true for NTD. In this work, we investigate how well current physical models can represent the experimental results obtained from actual NTD processes and what may cause the observed deviations.

2. Approach to modeling negative tone development

In positive tone development of standard chemically amplified photoresist, the polymer dissolution properties in aqueous base of the polymer increase as acid labile 'protecting' groups are removed from the polymer. These 'leaving' groups are 'de-protected' in an acid catalyzed reaction during the PEB (Post Exposure Bake) and volatilize out of the film. In the negative tone development process, a solvent developer is used; this exploits the fact that the polarity of the resist material increases with higher de-protection extent. As the polymer's polarity increases, its solubility in the solvent decreases. Because the entire chemistry of NTD and PTD seem nearly identical other than the direction of solubility on the development step, the obvious approach is to use the same chemically amplified resist model as currently employed for PTD but reverse the development rate equation. However, the evaporation of the leaving groups will also lead to shrinkage of the resist film which may have a significant impact on the final resist cross-section shape. After PEB and after develop resist thickness is shown in Figure 1 for a model NTD system from Dow [9]. As shown in the Figure, about 15nm of thickness loss is seen after PEB at high exposure dose values. After develop, an additional 15nm of resist loss is also observed. From this simple experiment, it is clear that accurate cross-section prediction will require both an accurate description of shrinkage during PEB and an accurate description of the develop process.

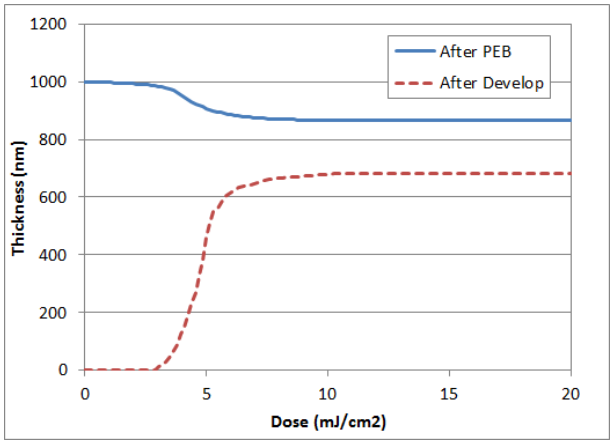

Figure 1: Resist thickness versus dose after PEB for a de-protecting photoresist for an open-frame exposure. The initial film thickness after spin-coat and soft bake was 100 nm. Also shown is the after-develop thickness with negative tone develop processing.

Our model for de-protection shrinkage follows the thermodynamic theory used by Flory [10] to describe deformation of a polymer with a solvent concentration. The mixture of polymer and solvent is a balance between the mechanical deformation of the polymer and the chemical interaction between a low-molecular weight solvent and the polymer. While polymer and solvent mixture may seem quite different from shrinkage during PEB, the same theoretical framework can be applied to shrinkage during the PEB process. In the current case, the product of the de-protection reaction acts as the low molecular weight solvent, and the photoresist resin acts as the polymer. Instead of the solvent penetrating the polymer and creating a deformed gel, our simulations represent the evaporation of the de-protection products to form a deformed photoresist structure. The theory starts with an equation for the free energy of the system:

$$F = F_{mix} + F_{elastic} \tag{1}$$

Where the first term is the free energy of mixing:

$$F_{mix} = k_B T\left(n_s \ln \phi_s + \chi n_s \phi_p\right) \tag{2}$$

Where k_B is Boltzmann's constant, T is temperature, n_s is the number of solvent molecules, ϕ_s and ϕ_p are the volume fraction of solvent and polymer, and χ is the Flory interaction parameter [10]. The second term in equation (1) is the contribution to the free energy due to deformation of the polymer network:

$$F_{elastic} = \frac{k_B T n_p}{2}\left(\alpha_1^2 + \alpha_2^2 + \alpha_3^2 - 3 - \ln \alpha_1\alpha_2\alpha_3\right) \quad (3)$$

Where n_p is the number of polymer molecules, and α_1, α_2, and α_3 are the eigenvalues of the finite strain tensor. We will not go into a detailed description of these free energy terms here, but the basic idea is that the system will reach equilibrium by minimizing the total free energy given by equation (1); this will require both chemical and mechanical equilibrium. The mixing term will cause a negative osmotic pressure as the blocking groups leave the polymer matrix, and this pressure term will be balanced by the elastic deformation of the polymer. We solve this mechanical problem using standard finite element techniques [11].

We further assume that the blocking groups volatilize out of the film during PEB, and that the density of the resist remains constant throughout the PEB process. As the film loses mass, the film must shrink to maintain constant density, and the shrinkage is linearly proportional to the local de-protection level. This is based on the protection level, M. It should be noted that the protection level in the remaining resist after development for NTD is much lower than PTD. We model this relationship by making the number of resist molecules a function of the local protection level:

$$n_p(M) = (n_{Max} - n_{Min})M + n_{Min} \quad (4)$$

Where n_{Max} and n_{min} are the maximum and minimum number of polymers in a unit volume within the resist. In an exposed area, protection level M will be lower, and because the leaving group has evaporated, the number of polymer molecules per unit volume will decrease to n_{min} because the leaving group acts like a solvent and dilutes the polymer concentration. This assumption allows the de-protection shrinkage to be inhomogeous over the resist domain. These two parameters can be obtained by fitting the PEB film shrinkage curve in Figure 1.

The second part of our model for NTD systems is the develop process. Several development rate equations [12-14] are routinely used in lithography simulation. The original equation proposed by Mack [12] is still the most commonly used. This rate equation given by:

$$R(M) = R_{Max}\frac{(a+1)(1-M)^n}{a+(1-M)^n} + R_{Min} \quad (5)$$

$$\text{and} \quad a = \frac{n+1}{n-1}(1-M_{th})^n$$

and $R(M)$ is the instantaneous bulk development rate, M is the local protection extent, R_{max} is the maximum development rate of the resist (when M = 0), R_{min} is the minimum development rate of the resist (when M = 1), n is the dissolution selectivity and M_{th} is the threshold protection level when there is an inflection point in the $R(M)$ curve.

This equation can be reversed to describe negative tone development by substituting $R(1\text{-}M)$ for $R(M)$. The meanings of R_{max} and R_{min} and n are retained, but the threshold protection level where the inflection in the development rate occurs is now at $1\text{-}M_{th}$. Figure 2 shows plots of the Mack model in both PTD and NTD modes. The R_{min} and R_{max} values were determined with a Develop Rate Monitor (DRM) for the model Dow material in PTD and NTD modes [9]. When the resist was developed as a positive tone material, R_{max} was larger than 290nm/sec (the resolution of the DRM) and R_{min} was very small (no detectable thickness change after 225 seconds for an unexposed sample). When the same material was developed with an organic solvent system, R_{max} was measured as 39.1nm/sec, and R_{min} was found to be 0.2nm/sec. This material demonstrates a typical trend with these materials: R_{max} is larger for PTD compared with NTD, and R_{min} is lower for PTD compared with NTD. This leads to lower develop contrast and greater thickness loss for the NTD system. This is all consistent with the results shown in Figure 1, where we show thickness after PEB and

after develop for an open frame exposure of an NTD system.

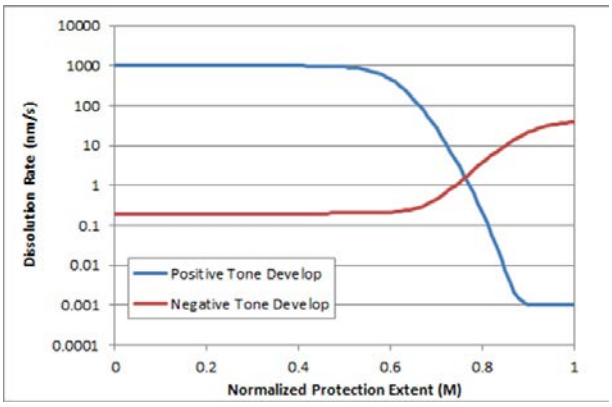

Figure 2: Plot of the Mack rate equation configured in both positive and negative tone dissolution modes, with measured maximum and minimum development rates for the model material in this study.

3. Results

Two cases are studied using the aforementioned NTD model. The focus of our study is on matching a simulated resist cross-section profile with an experimental result [15]. First, an isolated feature (100nm trench on 600nm pitch) is modeled and compared with experiment. Next, the same material model is applied to a second case where 65nm trench is on printed on a 130nm pitch. Again, the cross-section from simulation is compared with experimental result.

3.1 100nm trench on 600nm pitch

In this example, we exposed a 100nm trench on a 600nm pitch and collected a cross-section SEM image shown in Figure 3. The center of the resist is around 54nm thick and edge is around 70nm thick. Then, we simulate this isolated trench structure using PROLITH™ (KLA-Tencor, Milpitas, CA) NTD processing. We first simulate the resist profile without de-protection shrinkage. Figure 4 shows the simulated resist profile without de-protection shrinkage (1.35NA, immersion ArF, 0.9/0.6 Annular, X/Y polarization). The top surface is flat and resist thickness is around 90nm. The protection level inside the resist is shown in Figure 5. As shown in the Figure, the middle of the resist line has a lower protection level compared to the edge. As a result, we should expect more shrinkage in the center than the outer edge.

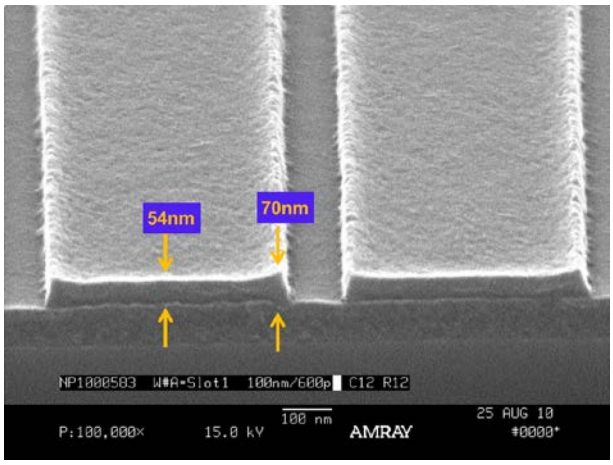

Figure 3: Electron microscopy cross-section shapes of resist lines in the case of 100nm isolated (600nm Pitch) trench (1.35NA, immersion ArF, 0.9/0.6 Annular, 21mJ/cm^2)

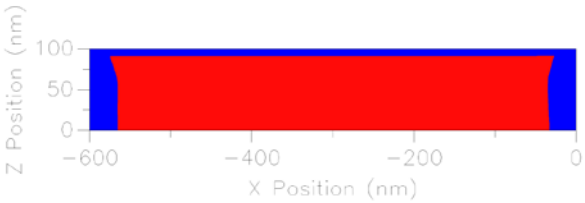

Figure 4: Simulated developed resist profile of 100nm isolated (600nm Pitch) trench without de-protection shrinkage

Figure 5: Simulated protection level in the resist feature in the case of 100nm isolated (600nm Pitch) trench (1.35NA, immersion ArF, 0.9/0.6 Annular, X/Y polarization) assuming typical generic model parameters.

Figure 6 shows the maximum principal stress in resist after PEB and de-protection shrinkage. The exposed area shows more shrinkage than unexposed area. The exposed part of the resist is found to be 85nm thick and the unexposed part is found to be 93nm thick. The whole resist is under tensile stress. It should be noted that the film thickness after PEB is higher than the final developed resist thickness at both the middle and the edge locations. The maximum stress is found in the

unexposed region which later would be developed away. It should be noted that the top of the resist is under higher stress than the bottom of the resist. As a result, during development the stress would be released and more vertical and lateral shrinkage would appear. Due to stress relaxation, the side-walls of resist are pulled in and the thickness of resist shrinks more. This phenomenon could be reproduced by simulation. After applying the shrinkage simulation on developed resist profile, the resist deforms and an updated resist profile is obtained and shown in Figure 7. It should be noted that the resist thickness is around 60nm in the middle of resist line and 70nm near the edge which is lower than the values in Figure 6 due to stress relaxation and development shrinkage. Compared to the simulated resist profile in Figure 4, the resist profile after shrinkage is a better match to the experiment result in Figure 3.

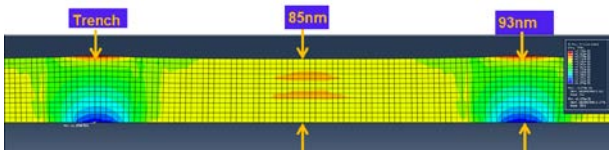

Figure 6: Maximum principal stress and resist thickness in resist film stack after PEB

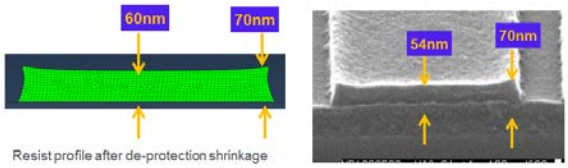

Figure 7: Simulated cross-section shape of resist lines for the case of 100nm isolated (600nm Pitch) trench after de-protection shrinkage (left) compared with experimental electron microscopy cross-section image of resist line (right).

3.2 65nm trench in 130nm pitch

In this example, we exposed a 65nm line on a 130nm pitch and collected the cross-sectional SEM (Scanning Electron Microscopy) image shown in Figure 8. The thickness of the developed resist feature is around 80nm, and the resist top is not as curved as the former case. This is due to lower de-protection level in dense feature. For comparison, we use PROLITH NTD processing to simulate the same structure. First, we simulate the resist profile without de-protection shrinkage, and we obtain a resist thickness of 93nm, as shown in Figure 9. In Figure 10, we show the protection level inside the resist. As for the isolated trench, the center of resist shows lower protection level compared to the edge. However, we can see that the protection level of dense feature from Figure 10 is higher than the protection level of isolated feature in Figure 5. We expect this will lead to a smaller amount of shrinkage in dense feature compared with the isolated case. Results of the de-protection shrinkage simulation are shown in Figure 11. Again, reasonable agreement between experiment and simulation is observed. The resist thickness shrinks down to 73nm from 93nm without shrinkage, compared to 68nm in the experimental SEM shown in Figure 8.

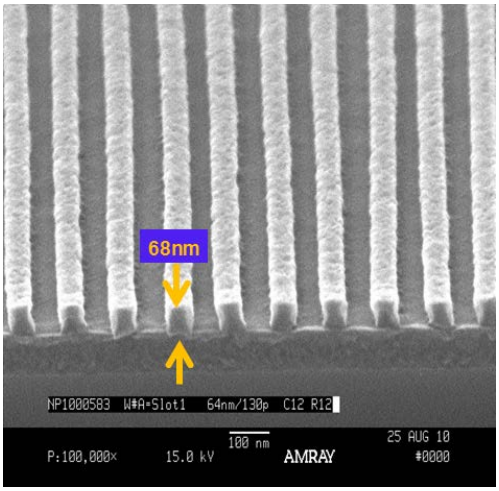

Figure 8: Electron microscopy cross-section shapes of resist lines in the case of 65nm dense (130nm Pitch) trench (1.35NA, immersion ArF, 0.9/0.6 Annular, X/Y polarization, 21mJ/cm^2)

4. Conclusions

Experimental NTD process data shows cross-sections that are often difficult to predict with conventional photolithography simulators. We have shown a new model for shrinkage of the resist during PEB that can be used in combination with accurate development rate data to predict NTD cross-sections. The amount of shrinkage varies locally according to the local protection level, which represents

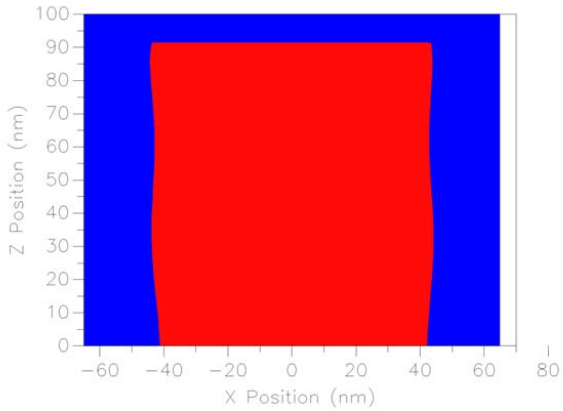

Figure 9: Final developed resist profile 65nm dense (130nm Pitch) trench without shrinkage

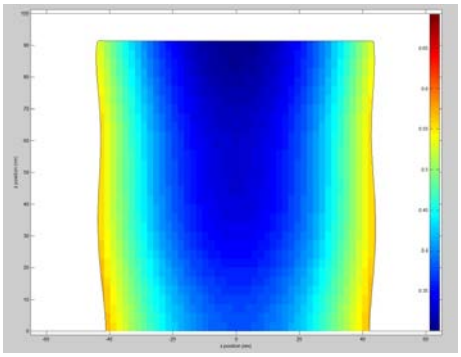

Figure 10: Protection level in the resist feature in the case of 65nm dense (130nm Pitch) trench (1.35NA, immersion ArF, 0.9/0.6 Annular, X/Y polarization) assuming typical generic model parameters.

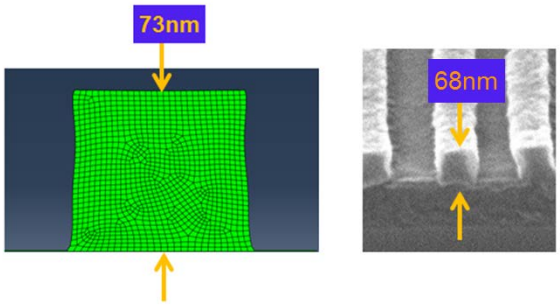

Figure 11: Simulated cross-section shape of a resist line in the case of 65nm isolated (130nm Pitch) trench after de-protection shrinkage (left) and electron microscopy cross-section image of resist line (right).

inhomogeneous material properties. Two examples are studied using our NTD model, and the simulated results were compared with experiments. We demonstrate the predictive capability of PROLITH NTD model on matching the resist cross-section shape for both isolated and dense cases using the same set of parameters.

Future work on this model will include exploration of shrinkage over multiple doses and focus conditions. Calibration using this model on more NTD resist material is also desirable for further validation.

5. Acknowledgement

The authors would like to thank Trey Graves for suggestions and help on generating simulation results. The authors also would like to thank Dow Electronic Materials and the PROLITH development team at KLA-Tencor, particularly David Blankenship, Timothy Yoas and Chris Walker.

References

1. Mack, C. A., Connors, J. E., “Fundamental differences between positive and negative tone imaging”, *Proc SPIE*, **1674** (1992) 1674328.
2. Pugliano, N., Bolton, P., Barbieri, T., Reilly, M., King, M., Lawrence, W., Kang, D., Barclay, G., “Negative tone 193 nm photoresists”, *Proc. SPIE*, **5039** (2003) 5039698.
3. Ando, T., Abe, S., Takasu, R., Iwashita, J., Matsumaru, S., Watababe, R., Hirahara, K., Suzuki, Y., Iwai, T., “Topcoat-free ArF negative tone resist”, *Proc SPIE*, **7273** (2009) 727308.
4. Tarutani, S., Hideaki, H., Kamimura, S., “Development of materials and processes for negative tone development towards 32-nm node 193-nm immersion double-patterning process”, *Proc. SPIE*, **7273** (2009) 72730C.
5. Tarutani, S., Kamimura, S., Yokoyama, J., “Process parameter influence to negative tone development process for double patterning”, Proc. SPIE, **7639** (2010) 76391Q.
6. Van Look, L., Bekaert, J., Truffert, V., Wiaux, V., Lazzarino, F., Maenhoudt, M., Vandenberghe, G., Reybrouck, M., Tarutani, S., “Printing the metal and contact layers for the 32 and 22 nm node: Comparing positive and negative tone development process”, *Proc. SPIE*, **7640** (2010) 764011.
7. Bekaert, J., Van Look, L., Truffert, V., Lazzarino, F., Vandenberghe, G., Reybrouck, M., Tarutani, S., “Comparing positive and

negative tone development process for printing the metal and contact layers of the 32- and 22-nm nodes", *J. Micro/Nanolith. MEMS MOEMS*, **9**(4), (2010) 10.

8. Mack, C. A., "Thirty years of lithography simulation", *Proc. SPIE*, **5754** (2005) 5754XVIII.
9. Robertson, S. A., Reilly, M., Biafore, J. J., Smith, M. D., Bae, Y. "Negative tone development: gaining insight through physical simulation," *Proc. SPIE*, **7972** (2011) 79720Y.
10. Flory, P. J., *Principles of Polymer Chemistry*, Cornell University Press (1953)
11. Thomas J.R. Hughes., *The Finite Element Method: Linear Static and Dynamic Finite Element Analysis*, Dover Civil and Mechanical Engineering (2000)
12. Mack, C. A., "Development of positive photoresist", *J. Electrochemical Society*, **134** (1) (1987) 148
13. Mack, C., A., "New kinetic model for resist dissolution", *J. Electrochemical Society*, **139** (4) (1992) L35.
14. Arthur, G., Mack, C., A., Martin, B., "A new development model for lithography simulation", *Proc Olin Microlithography Seminar Interface* '97, pp 55, (1997)
15. Robertson, S., Reilly, M., Bae, Y., "Physical resist simulation for a negative tone development process," SEMATECH *International Symposium on Lithography Extensions*, Kobe, Japan (2010).